Quantum description of light-pulse scattering on a single atom in waveguides

Peter Domokos,* Peter Horak,† and Helmut Ritsch
Institut for Theoretical Physics, Universität Innsbruck, Technikerstrasse 25, A-6020 Innsbruck, Austria
(Received 26 November 2001; published 1 March 2002)

We present a time-dependent quantum calculation of the scattering of a few-photon pulse on a single atom. The photon wave packet is assumed to propagate in a transversely strongly confined geometry, which ensures strong atom-light coupling and allows a quasi-one-dimensional treatment. The amplitude and phase of the transmitted, reflected, and transversely scattered part of the wave packet strongly depend on the pulse length (bandwidth) and energy. For a transverse mode size of the order of λ^2, we find nonlinear behavior for a few photons already, or even for a single photon. In a second step we study the collision of two such wave packets at the atomic site and find striking differences between the Fock state and coherent state wave packets of the same photon number.

DOI: 10.1103/PhysRevA.65.033832 PACS number(s): 42.50.Ct, 42.65.−k, 42.82.−m

I. INTRODUCTION

Identifying and realizing systems with strong coupling between light and matter is one of the central objectives of current research in quantum optics. In the strong-coupling regime the coherent interaction between a few atoms and the radiation field of few photons takes place on a fast time scale and is not masked by the dissipative coupling to the environment. A weak quantum field can change the internal quantum state of an atom and, vice versa, a single atom is able to have an appreciable influence on the light field. Both effects have, evidently, many interesting practical implications including single-atom detectors as well as nonlinear micro-optical elements on the single-photon level, which are in the heart of all-optical quantum information processing schemes [1], e.g., to facilitate Bell state detectors for photons [2].

So far optical experiments in the strong-coupling regime have been performed with atoms put in tiny high-Q cavities [3,4]. Here the origin of the strong coupling is the small volume of the discrete cavity modes. The local electric field sustained by a single photon becomes then very large. Strong coupling in the microwave regime yielded several spectacular results [5,6]. However, the electric field enclosed in three dimensions allows only limited accessibility, which complicates direct detection of the light and limits the time scales. In addition, the scalability to a large number of such elements seems rather difficult.

Hence, there is still a high demand for alternative setups that allow controlled manipulation and strong (nonlinear) coupling of single photons. It seems natural to try to lift the confinement of the light field in one particular dimension and consider the interaction of transversely confined propagating fields with nonlinear optical elements. If a photon forms a very short wave packet along its propagating direction, we again get a small total volume and a high field per photon. Conceptually the most simple nonlinear element for such wave packets is, of course, a single atom with a resonant dipole transition. An atomic dipole can be associated with an effective radiative cross section of $\sigma_A = 3\lambda^2/2\pi$. Hence, as a first guess one would expect that it is sufficient to simply focus a light beam down to a cross section of the same order of magnitude as σ_A to enter the strong-coupling regime. This is not too restrictive, as beams can be focused down to a spot size smaller than λ^2. Unfortunately, this line of argumentation is too naive and a precise calculation for such a strongly focused beam shows that the light will propagate through the atom without being noticeably influenced [7]. The reason for this can be traced back to the large range of transverse wave vectors involved in the dynamics yielding rapid variation of input phase and polarization. Another way to enhance the effective atomic cross section could, in principle, consist in using a quantum degenerate gas as an optically dense medium [8]. Here the use of many atoms leads to quite stringent practical limitations.

It is the advent of highly developed nanofabrication techniques that may open the way to new geometries avoiding these problems and facilitating setups to implement quasi-one-dimensional scattering processes on dipoles. Miniaturized waveguides on surfaces or optical fibers can be fabricated with cross sections of the order of the optical wavelength square. Photons traveling within are well confined in the transverse direction, while the field remains uniform in the longitudinal direction of propagation. The problems of the beam divergence and rapidly varying wave vector, encountered in free space, are missing in the waveguide setup. Hence one can hope that a single atom placed in the field of such a mode will have considerable influence on the dynamics. The investigation of the prospects of such a setup is the subject of the present paper.

We will study the time-dependent interaction of an atomic point dipole modeled by a two-level atom and the quantized electromagnetic field in a single transverse mode waveguide. We use the term ''waveguide'' in a general sense, avoiding any precise geometric specification. Instead, we set up a model that accounts for the generic features of these devices. The central property is that the atom interacts with a continuum of transversally confined propagating modes. A simi-

*On leave from Research Institute for Solid State Physics and Optics, Budapest, Hungary.
Electronic address: Peter.Domokos@uibk.ac.at
†Present address: Optoelectronics Research Centre, University of Southampton, United Kingdom.

lar system has been studied to investigate the influence of input photon statistics on single-atom absorption [9]. For this the theory of cascaded open systems [10,11] as an extended form of the input-output formalism was applied. In contrast to the stationary scattering scenario, we will concentrate here on the time-dependence of the scattering process, i.e., we consider *wave packets* consisting of one or a few photons impinging on an atom. This allows one to find the dependence of the atomic dynamics and the amount of scattering on the light pulse bandwidth and energy beyond the narrow-bandwidth limit considered in Ref. [9]. For very short pulses, the energy of a single photon is strongly concentrated in space and thus saturation is expected to prominently influence the scattering process even for weak energy incident wave packets. As a consequence, we have to take the full quantum dynamics of the dipole into account, including saturation to all orders.

To treat this problem of wave-packet scattering, we develop a method based on a set of Heisenberg-Langevin equations for the field and atomic operators. These equations, relying on first principles of quantum mechanics, will be transformed into a simplified form by means of a Markoff approximation. This approximation closely relates our approach to the cascaded open systems method. Nevertheless we are primarily interested in the field dynamics, called ''channel'' in the scheme of cascaded systems. Hence we will keep the waveguide electric field as an explicit dynamic component of our model. Let us mention here that some numerical examples calculating the electric field of the propagation of a single-photon wave packet through a single atom have been obtained before [12]. Similarly the dynamics of a two-dimensional (2D) one-photon wave packet and many two-state atoms modeling a beam splitter was numerically solved [13].

Nevertheless, the systematic and exhaustive discussion of the parameter space by a purely numerical approach seems hopeless. Fortunately, in our method, we are able to get explicit analytical expressions for the scattered waveguide field. This result exhibits the scaling with the ratio of the transverse mode size and the atomic cross section. Thus we can easily reveal how this ratio governs the energy redistribution in a scattering process. In addition, physical insight in the phase properties and the pulse-shape deformation can also be gained.

As a possible application of our model we address the problem of atom-mediated nonlinear photon-photon interaction. So far, significant coupling has been reached with the help of a high-Q cavity [14] or might be reached by increasing the number of atoms [8,15]. The waveguide-atom interaction could be the basis of nonlinear pulse amplifiers or even that of photonic quantum gates. Here we limit the study to a prototype interference experiment in which two wave packets impinge simultaneously on the same atom.

The paper is organized as follows. In Sec. II we present the model and introduce the basic parameter describing the coupling of the atomic dipole and the waveguide, and finally, calculate the scattered electric field generally within a Markoff approximation. In Sec. III the transmitted and reflected Poynting vectors are studied for various initial states of the wave packet. These states include coherent states and the single-photon Fock state. We study the role of the pulse bandwidth in the scattering process and the saturation nonlinearity for multiphoton wave packets. The phase properties and the pulse-shape deformation is also discussed in this section. Then, Sec. IV is devoted to the interaction of light pulses. We conclude finally in Sec. V.

II. THE MODEL

Let us consider a single branch of modes propagating in the $+z$ direction of a lossless waveguide. The longitudinal wave number k of the modes is assumed to obey the simple dispersion relation $k=\omega/c$, which is valid far from the branch threshold [16]. The effective transverse cross section of the modes

$$\mathcal{A}=\frac{\int dx\,dy|f_k(x,y)|^2}{|f_k(x_a,y_a)|^2},$$

where $f_k(x,y)$ is the transverse mode function and (x_a,y_a) is the position of the atom, is approximately constant in the range of the relevant longitudinal wave numbers. The details of the transverse mode profile do not play an important role in the forthcoming calculations as long as the atom may be treated as pointlike. Only the value of the mode function at the position of the atom enters in the calculation. This value has been incorporated in the definition of the effective cross section $\mathcal{A}$. Similarly, the polarization properties of the field can also be omitted provided the field is closely uniform across the spatial wave function of the atom. No assumption is made on the atomic position relative to the waveguide. In principle, the atom can sit inside a hollow waveguide, it can be embedded in the dielectric material of a fiber or can be even outside a dielectric interacting with the evanescent field close to the surface.

The continuum field quantization follows the theory presented in Ref. [17]. The electric radiation field is decomposed into positive- and negative-frequency parts

$$E(z,t)=E^{(+)}(z,t)+E^{(-)}(z,t), \tag{2.1}$$

where

$$E^{(+)}(z,t)=i\int_0^\infty d\omega\sqrt{\frac{\hbar\omega}{4\pi\epsilon c\mathcal{A}}}\{a_\omega(t)\exp[-i\omega(t-z/c)] + b_\omega(t)\exp[-i\omega(t+z/c)]\}. \tag{2.2}$$

We separated the modes of the two counterpropagating directions into sets a_ω and b_ω—the first corresponding to the forward and the latter to the backward propagating modes. The electric field is given in the interaction picture. The field-amplitude variables $a_\omega(t)$ and $b_\omega(t)$ describe then the time variation due to the interaction with the atom. They follow the usual bosonic commutation rules

$$[a_\omega(t),a^\dagger_{\omega'}(t)]=[b_\omega(t),b^\dagger_{\omega'}(t)]=\delta(\omega-\omega'), \tag{2.3}$$

all the other commutators vanish.

The atomic dipole, again in interaction picture, reads

$$d = d_{eg}(\sigma_- e^{-i\omega_A t} + \sigma_+ e^{i\omega_A t}), \tag{2.4}$$

where the operators $\sigma_\pm$ together with $\sigma_z = (\sigma_+\sigma_- - \sigma_-\sigma_+)/2$ form a pseudospin obeying the spin-$\frac{1}{2}$ algebra. We assume that the dipole moment is oriented parallel to the field polarization at the atomic position yielding maximum coupling.

The dipole interaction Hamiltonian in the rotating-wave approximation is given by

$$H_I = -i\hbar \int d\omega g_\omega [\sigma_+ (a_\omega e^{i\omega z_A/c} + b_\omega e^{-i\omega z_A/c}) \times e^{-i(\omega-\omega_A)t} - \text{H.c.}], \tag{2.5}$$

where z_A is the position of the atom, and the coupling constants are

$$g_\omega = \sqrt{\frac{\omega}{4\pi\epsilon\hbar c\mathcal{A}}} d_{eg}. \tag{2.6}$$

Note that the dimension of the coupling constant g_ω is not a frequency but $1/\sqrt{\text{sec}}$. The use of the rotating-wave approximation is justified as we consider light pulses with a bandwidth much smaller than the frequency ω_A.

The evolution of the system variables is governed by a set of coupled Heisenberg-Langevin equations [18]

$$\frac{d}{dt} a_\omega = g_\omega \sigma_- e^{-i\omega z_A/c} e^{i(\omega-\omega_A)t}, \tag{2.7a}$$

$$\frac{d}{dt} b_\omega = g_\omega \sigma_- e^{i\omega z_A/c} e^{i(\omega-\omega_A)t}, \tag{2.7b}$$

$$\frac{d}{dt}\sigma_- = -\gamma_0\sigma_- + 2\sigma_z \int d\omega g_\omega \times (a_\omega e^{i\omega z_A/c} + b_\omega e^{-i\omega z_A/c}) e^{-i(\omega-\omega_A)t} + \hat{\xi}_-, \tag{2.7c}$$

$$\frac{d}{dt}\sigma_z = -2\gamma_0(\sigma_z + 1/2) - \int d\omega g_\omega [\sigma_+ (a_\omega e^{i\omega z_A/c} + b_\omega e^{-i\omega z_A/c}) \times e^{-i(\omega-\omega_A)t} + \text{H.c.}] + \hat{\xi}_z. \tag{2.7d}$$

Besides the terms originating from the interaction Hamiltonian (2.5), we account for the interaction of the atom with an environment. This coupling results in a dissipation process with decay rate γ_0 and with associated noise represented by the operators $\hat{\xi}$. The physical role of this γ_0 decay process is that it provides a channel for the transverse scattering, i.e., when photons are scattered by the atom out of the waveguide. The environment consists of the free-space radiation modes [21]. Of course, the presence of the 1D waveguide slightly perturbs the surrounding mode structure with respect to the simple free-space case. This effect, which depends on the specific choice of the waveguide geometry, is neglected and, for the sake of simplicity, in the numerical examples we will use the free-space spontaneous decay rate $\gamma_0 = \omega_A^3 d_{eg}^2/(6\pi\epsilon_0\hbar c^3)$.

The waveguide modes form a one-dimensional continuum. The above equations can be transformed then into a much simpler form by means of a Markoff approximation. On integrating Eq. (2.7a), the waveguide-field amplitudes arise in a form decomposed into a free field part and into a part radiated by the atom [18]

$$a_\omega(t) = a_\omega(t_0) + g_\omega e^{-i\omega z_A/c} \int_{t_0}^{t} dt' \sigma_-(t') e^{i(\omega-\omega_A)t'}, \tag{2.8}$$

respectively. The back-propagating modes are decomposed analogously. The Markoff approximation is invoked to describe the back action of the second term on the atom. It can be applied because the continuum is broadband around the atomic frequency. The free-field term is usually identified with a Langevin-type noise source. In the waveguide we cannot make this step, since we will consider initial field states different from the vacuum. Altogether, the atom is subject to the effect of the free field and to a relaxation into the waveguide continuum. The polarization operator σ_-, for example, follows

$$\frac{d}{dt}\sigma_- = -(\gamma_0+\gamma_1)\sigma_- + 2\sigma_z \int d\omega g_\omega [a_\omega(t_0) e^{i\omega z_A/c} + b_\omega(t_0) e^{-i\omega z_A/c}] e^{-i(\omega-\omega_A)t} + \hat{\xi}_-, \tag{2.9}$$

where a new damping rate γ_1 appears, and the second term contains the free-field contributions. The vacuum frequency shift induced by the waveguide modes, accompanying the relaxation, is assumed to be already incorporated in a renormalized atomic frequency ω_A. The rate of spontaneous emission into the waveguide modes is given by

$$\gamma_1 = 2\pi g_{\omega_A}^2 = \frac{1}{2}\frac{\sigma_A}{\mathcal{A}}\gamma_0, \tag{2.10}$$

where the second expression directly exhibits the scaling with the transverse extension of the waveguide. It is related to the atomic radiative cross section $\sigma_A = 3\lambda^2/2\pi$. A natural lower bound on the transverse mode size is at about $\mathcal{A} \sim (\lambda/2)^2$ (cf. lowest-order mode in hollow metallic waveguide), implying a maximum achievable coupling ratio $\gamma_1/\gamma_0 \sim 1$. In the range $\sigma_A \sim \mathcal{A}$, one has a strong waveguide-atom coupling, which is manifested by the fact that the atom dissipates its energy equally into the waveguide and the free-space ''lossy'' modes. This situation could turn out to be a suitable basis to construct single-atom detectors or efficient light-emitting diodes.

For the following, it is convenient to introduce the ''free-pulse'' operators

$$g_{\omega_0} a_0(t) = \int_0^\infty d\omega g_\omega a_\omega(t_0) e^{-i(\omega-\omega_0)t}, \tag{2.11}$$

and the same for $b_0(t)$, where ω_0 can be any frequency and will later be identified with the central frequency of the wave packet. The evolution of the atomic operators is given by the equations

$$\frac{d}{dt}\sigma_- = -\gamma\sigma_- + 2\sigma_z g_{\omega_0}[a_0(t-z_A/c)e^{i\omega_0 z_A/c} + b_0(t+z_A/c)e^{-i\omega_0 z_A/c}]e^{-i(\omega_0-\omega_A)t} + \hat{\xi}_- \tag{2.12a}$$

$$\frac{d}{dt}\sigma_z = -2\gamma(\sigma_z+1/2) - g_{\omega_0}\{\sigma_+[a_0(t-z_A/c)e^{i\omega_0 z_A/c} + b_0(t+z_A/c)e^{-i\omega_0 z_A/c}]e^{-i(\omega_0-\omega_A)t} + \text{H.c.}\} + \hat{\xi}_z, \tag{2.12b}$$

where $\gamma=\gamma_0+\gamma_1$ is the total decay rate of the atomic dipole. This is the generalization of the Bloch equations for the atomic dipole operators to describe the effect of a time-dependent external excitation in the case of a quantum driving field. For certain quantum states of the field, a closed set of equations can be derived from the above operator equations to calculate the matrix elements of the atomic operators. Note that only the free field appears in the dynamics of the atomic-dipole operators. This is a direct consequence of the Markoff approximation, which implies that any change of the electromagnetic field by the atom cannot act back onto the atom. In other words, a photon emitted by the atom into the waveguide leaves the interaction region immediately and cannot be reabsorbed. There is no feedback mechanism as provided by the mirror in cavities. Hence the strong coupling between the atom and waveguide yields a different dynamics with respect to the case of ordinary cavity QED.

On inserting the solution of Eq. (2.12a) into Eq. (2.8), the field operator can be obtained in the form

$$a_\omega(t) = a_\omega(t_0) + a_\omega^{\text{scat}}(t) + a_\omega^{\text{back}}(t) + a_\omega^{\text{rad}}(t) + a_\omega^{\text{noise}}(t), \tag{2.13}$$

where the five terms represent, respectively, the free field, the field forward and backward scattered by the atom, the field radiated by an initially excited atom, and finally the vacuum noise that is coupled into the waveguide via the atomic dipole. They read

$$a_\omega^{\text{scat}}(t) = g_\omega g_{\omega_0} e^{-i(\omega-\omega_0)z_A/c}\int_0^t dt' e^{i(\omega-\omega_A+i\gamma)t'} \times \int_0^{t'} dt'' e^{-i(\omega-\omega_A+i\gamma)t''} 2\sigma_z(t'')a_0(t''-z_A/c), \tag{2.14a}$$

$$a_\omega^{\text{back}}(t) = g_\omega g_{\omega_0} e^{-i(\omega+\omega_0)z_A/c}\int_0^t dt' e^{i(\omega-\omega_A+i\gamma)t'} \times \int_0^{t'} dt'' e^{-i(\omega-\omega_A+i\gamma)t''} 2\sigma_z(t'')b_0(t''+z_A/c), \tag{2.14b}$$

$$a_\omega^{\text{rad}}(t) = g_\omega e^{-i\omega z_A/c}\int_0^t dt' \exp[i(\omega-\omega_A+i\gamma)t']\sigma_-(t_0), \tag{2.14c}$$

$$a_\omega^{\text{noise}}(t) = g_\omega e^{-i\omega z_A/c}\int_0^t dt' \times \exp[i(\omega-\omega_A+i\gamma)t']\int_0^{t'} dt'' e^{\gamma t''}\hat{\xi}_-(t''). \tag{2.14d}$$

We have set the initial time $t_0=0$. Nevertheless, we still will use t_0 sometimes in order to explicitly mark the initial value of the operators evolving in the Heisenberg picture. In the double-time integrals, the order can be exchanged to carry out one of them. Substituting the solution in the electric-field decomposition (2.2), the integral over the frequency ω can also be performed. In this latter step, the lower bound of the frequency integration is extended to $-\infty$. For $ct>z-z_A$, i.e., a light pulse has enough time to travel to the atom, one finds the following result for the waveguide electric field in the half space $z>z_A$:

$$E^{(+)}(\tau) = i\sqrt{\frac{\hbar\omega_0}{4\pi\epsilon c\mathcal{A}}}e^{-i\omega_0\tau}\Bigg[a_0(\tau) + \frac{1}{2}\frac{\sigma_A}{\mathcal{A}}\gamma_0\int_0^{\tau+z_A/c}dt' \exp[i(\omega_0-\omega_A+i\gamma)(\tau+z_A/c-t')]2\sigma_z(t')a_0(t'-z_A/c) + \frac{1}{2}\frac{\sigma_A}{\mathcal{A}}\gamma_0 e^{-2i\omega_0 z_A/c}\int_0^{\tau+z_A/c}dt' \exp[i(\omega_0-\omega_A+i\gamma)(\tau+z_A/c-t')]2\sigma_z(t')b_0(t'+z_A/c)\Bigg] + i\sqrt{\frac{\hbar\omega_A}{4\pi\epsilon c\mathcal{A}}}2\pi g_{\omega_A}\exp[-(i\omega_A+\gamma)(\tau+z_A/c)]\Bigg[\sigma_-(t_0) + \int_0^{\tau+z_A/c}dt' e^{\gamma t'}\hat{\xi}_-(t')\Bigg], \tag{2.15}$$

where $\tau=t-z/c$, and only the modes a_ω are considered as we are interested in the field outgoing in the $+z$ direction ($z>z_A$). In the subsequent terms one gets the free, the forward, the backward scattered, then the directly radiated and finally the noise field. This is the central result that we use in the following to calculate measurable quantities in various experimental scenarios. One can draw a general conclusion already at this stage that the scattered terms are proportional, as naively expected, to the ratio $\sigma_A/\mathcal{A}$.

III. SCATTERING OF A SINGLE LIGHT PULSE

In this section we study the scattering process of a single light-wave packet off a ground-state atom. We calculate how the photons carried by the wave packet are redistributed among the forward, backward, and transverse directions. The relevant quantity to be calculated is the expectation value of the Poynting vector defined as

$$S(z,t)=\frac{\mathcal{A}}{\hbar\omega_0}\frac{1}{\mu_0}\langle\Psi_0|B^{(-)}E^{(+)}+E^{(-)}B^{(+)}|\Psi_0\rangle, \tag{3.1}$$

given in units of photon current in the forward and backward direction after the scattering event. In the present scalar model the magnetic field is just proportional to the electric field. The initial state $|\Psi_0\rangle$ is a simple product state of the waveguide field state, the atomic ground state, and the environment

$$|\Psi_0\rangle=|\psi_a\rangle|0_b\rangle|g\rangle|0_e\rangle. \tag{3.2}$$

The waveguide field describes a wave packet propagating in the direction $+z$, i.e., only the modes a_ω are excited with state $|\psi_a\rangle$, while the counterpropagating modes b_ω are in vacuum state $|0_b\rangle$. As for the initial state $|\psi_a\rangle$ we will use Fourier-transform-limited Gaussian pulses in a coherent state or in a single-photon Fock state, respectively. The mean Poynting vector of a free pulse is then

$$S_0(z,t)=N_a\frac{\Omega}{\sqrt{2\pi}}\exp\left[-\frac{1}{2}\Omega^2(t-z/c)^2\right], \tag{3.3}$$

where N_a is the mean photon number carried by the wave packet and Ω is the pulse bandwidth.

As no field is radiated from an atom in the ground state, there is no contribution from the fourth term of Eq. (2.15) to the Poynting vector. Similarly the free-space environment as well as the backward-propagating modes are in vacuum state. Therefore, all the terms containing the noise operator $\hat{\xi}_-$ or $b_\omega(t_0)$ on the right-most side will vanish acting on the initial state $|\Psi_0\rangle$. Thus the mean Poynting vector in the forward direction $z>z_A$ is formed from the superposition of the original light pulse and the one forward scattered by the atom

$$\begin{aligned}S(\tau)=\frac{\Omega}{\sqrt{2\pi}}e^{-\Omega^2\tau^2/2}\Bigg[&\langle u(\tau)|u(\tau)\rangle+\frac{\sigma_A}{\mathcal{A}}\gamma_0\int_0^{\tau+z_A/c}dt'\ \mathrm{Re}\{\mathcal{F}(\tau,t')\langle u(\tau)|2\sigma_z(t')|u(t'-z_A/c)\rangle\}\\&+\left(\frac{\sigma_A}{2\mathcal{A}}\gamma_0\right)^2\int_0^{\tau+z_A/c}dt'\mathcal{F}^*(\tau,t')\int_0^{\tau+z_A/c}dt''\mathcal{F}(\tau,t'')\langle u(t'-z_A/c)|4\sigma_z(t')\sigma_z(t'')|u(t''-z_A/c)\rangle\Bigg],\end{aligned} \tag{3.4}$$

where $\tau=t-z/c$ and

$$\begin{aligned}\mathcal{F}(\tau,t')=\exp\Bigg(&\frac{\Omega^2}{4}(\tau+t'-z_A/c)(\tau+z_A/c-t')\\&+i(\omega_0-\omega_A+i\gamma)(\tau+z_A/c-t')\Bigg).\end{aligned} \tag{3.5}$$

The Poynting vector is expressed in a product form with the original pulse-shape function separated in a first term. To this end, we defined an auxiliary state

$$|u(t)\rangle=(2\pi\Omega^2)^{-1/4}e^{\Omega^2t^2/4}a_0(t)|\Psi_0\rangle. \tag{3.6}$$

As we work in the Heisenberg picture, the time dependence of this auxiliary state does not describe a dynamical process but follows from its definition.

The reflected field in the domain $z<z_A$ results from the light backscattered by the atom (and additional quantum noise). As for the atomic radiation the two directions in the waveguide are equivalent, one gets an expression formally identical to the third term of Eq. (3.4)

$$\begin{aligned}S^{(\mathrm{back})}(\tau')=&\frac{\Omega}{\sqrt{2\pi}}e^{-\Omega^2\tau'^2/2}\left(\frac{\sigma_A}{2\mathcal{A}}\gamma_0\right)^2\\&\times\int_0^{\tau'+z_A/c}dt'\mathcal{F}^*(\tau',t')\int_0^{\tau'+z_A/c}dt''\mathcal{F}(\tau',t'')\\&\times\langle u(t'-z_A/c)|4\sigma_z(t')\sigma_z(t'')|u(t''-z_A/c)\rangle,\end{aligned} \tag{3.7}$$

where $\tau'=t-(2z_A-z)/c$, expressing that the field propagates now in the $-z$ direction.

A. Coherent-state light pulse

In the following, we present how to evaluate the Poynting vector (3.4) in the case of wave packets initially in a coherent state. A definition of multimode coherent-state pulses can be found in Ref. [17]. They have the property that they are eigenstates of the annihilation operators. A coherent-state pulse of bandwidth Ω, centered initially at $z=0$, can be defined through the eigenvalue equation

$$a_\omega(t_0)|\psi_a\rangle=\sqrt{N_a}\left(\frac{2}{\pi\Omega^2}\right)^{1/4}\exp[-(\omega-\omega_0)^2/\Omega^2]|\psi_a\rangle, \tag{3.8}$$

where N_a is the initial mean photon number in the wave packet. Its photon statistics is Poissonian around the mean N_a with variance $\sqrt{N_a}$.

It follows that $|\Psi_0\rangle$ is an eigenstate of the free-pulse operator $a_0(t)$ and we have

$$|u(t)\rangle = \sqrt{N_a}|\Psi_0\rangle. \tag{3.9}$$

To evaluate the Poynting vector Eq. (3.4), we need the one-time and the two-time averages of the population inversion operator. An equation of motion for $\langle\sigma_z(t)\rangle$ can be directly obtained by taking the mean of the Eqs. (2.12). Using again that $|\Psi_0\rangle$ is an eigenstate of the free-pulse operators, the usual form of the optical Bloch equations is found. We present it in the Appendix. However, when the evolution of $\langle\sigma_z(t)\sigma_z(t')\rangle$ as a function of t is calculated from Eq. (2.12), the operator $\sigma_z(t')$ stands in between the free-pulse operator and the state $|\Psi_0\rangle$. We prove in the same Appendix that $a_0(t-z_A/c)$ and $\sigma(t')$ commute for $t>t'$ and, therefore, the action of the pulse operator on its eigenstate can be easily carried out. This lemma allows the use of a form of the quantum regression theorem to calculate the two-time average $\langle\sigma_z(t)\sigma_z(t')\rangle$.

As it is shown in the Appendix, an effective single-photon Rabi frequency $g_{\rm eff}=g_{\omega_0}(2\pi\Omega^2)^{1/4}$ can be identified in the Bloch equations. This coupling constant suggests that the wave packet has an effective "volume" of $\sqrt{2\pi}c\mathcal{A}/\Omega$. For larger bandwidths Ω, we get a stronger field per photon, which is a central quantity in cavity QED. However, the interaction time between the atom and the transform-limited pulses gets simultaneously shorter, limiting the possibility of coherent operations on the atomic states.

The photon number N_a multiplies all the terms in the Poynting vector (3.4). Beyond this simple linear dependence, the photon number has an influence on the evolution of the atomic population. Through this term, the atomic saturation introduces a nonlinear behavior into the Poynting vector, which can be a noticeable effect in the strong-coupling regime even for relatively small photon numbers N_a.

B. Fock-state light pulse

Now let us turn to a second example and study a wave packet of precisely one photon. The single-photon Fock state is defined by

$$|1_a\rangle = \int_0^\infty d\omega \left(\frac{2}{\pi\Omega^2}\right)^{1/4} \exp[-(\omega-\omega_0)^2/\Omega^2] a_\omega^\dagger(t_0)|0_a\rangle. \tag{3.10}$$

The definition in Eq. (3.6) leads to

$$|u(t)\rangle = |0_a\rangle|0_b\rangle|g\rangle|0_e\rangle, \tag{3.11}$$

which, similar to the coherent-state case Eq. (3.9), is time independent. We now need the diagonal matrix elements $\langle 0,g|\sigma_z(t)|0,g\rangle$ and $\langle 0,g|\sigma_z(t)\sigma_z(t')|0,g\rangle$ where 0 stands for both modes a and b and for the environment. Equation (2.12) implies that $\langle 0,g|\sigma_z(t)|0,g\rangle = -1/2$ for arbitrary time t. In fact, this value is the initial condition itself that makes the right-hand side of the generalized Bloch equations vanish. Using again the commutation of the operators $a_0(t-z_A/c)$ and $\sigma(t')$, one can show that $\langle 0,g|\sigma_z(t)\sigma_z(t')|0,g\rangle = 1/4$ independently of t and t'. We get such simple solutions because we consider, formally, the Bloch equations when the atom is driven by a "vacuum pulse."

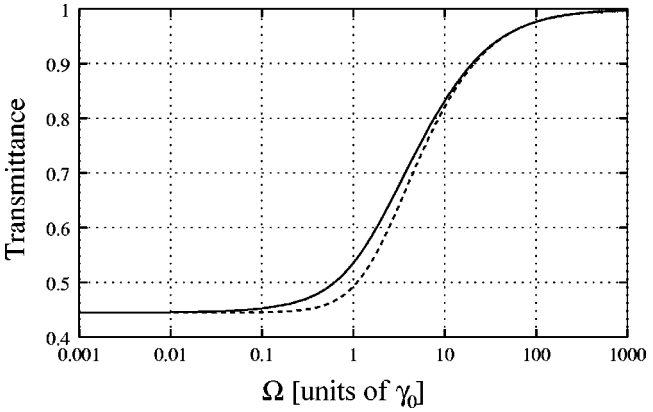

FIG. 1. Resonant single-atom transmittance as a function of the pulse bandwidth for pulses initially in coherent state with mean photon number $N_a=1$ (solid line) and in single-photon Fock state (dashed line). The parameters are $\omega_A=\omega_0$ (resonant pulse) and $\sigma_A=\mathcal{A}$.

Having the exact solutions for the one-time and two-time averages, the integrals in Eq. (3.4) can be analytically evaluated. The integration invokes the complex error function and the result itself is not very instructive. We omit this rather long formula here and only show typical results graphically in the figures of the following section.

C. Single-atom transmittance and reflectance

We continue the discussion of light-pulse scattering on a single atom by means of numerical examples. For this we evaluate the Poynting-vector expressions (3.4) and (3.7) to determine how much of a light pulse is transmitted and reflected back by the atom. We introduce the transmittance, i.e., the transmitted mean energy (photon number) divided by the mean energy of the impinging wave packet. For an atom being on resonance with the pulse-carrier frequency $\omega_A=\omega_0$, we expect the strongest scattering. In the forthcoming examples the waveguide cross section is set to $\sigma_A=\mathcal{A}$.

In Fig. 1 the single-atom transmittance is presented as a function of the pulse bandwidth on a logarithmic scale.

The overall shape of the transmittance curve is very similar for a pulse initially in a coherent state with $N_a=1$ (solid line) or if it is in a single-photon Fock state (dashed line). The difference is manifest for bandwidths close to the transition linewidth, $\Omega\approx\gamma_0$. Apparently the effective saturation is reduced if exactly one photon is present instead of a distribution with mean one.

As the incoming mean photon number is now 1 in this example, the transmittance gives directly the mean transmitted photon number. The atom presents an "obstacle" provided the pulse length is of the order of the natural lifetime

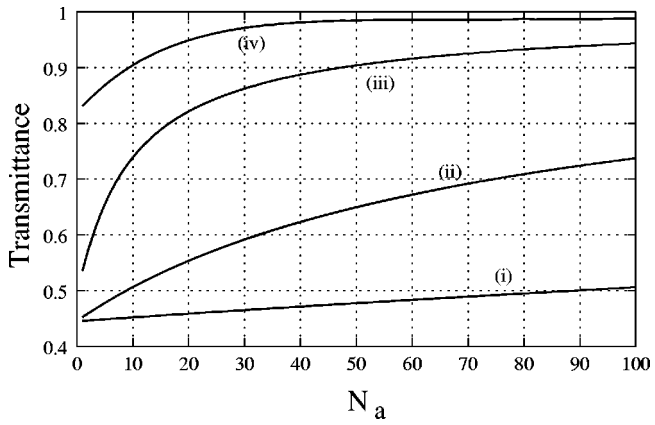

FIG. 2. Transmittance as a function of the mean photon number N_a of the initial coherent-state pulse. Curves (i), (ii), (iii), and (iv) are associated with the pulse bandwidths $\Omega=\gamma_0/100$, $\gamma_0/10$, γ_0, and $10\gamma_0$, respectively.

or longer, i.e., for $\Omega<\gamma_0$. The single-atom effect on the transmittance is approximately constant up to pulse lengths of few times the atomic lifetime. In this range the transmitted power is less than the half of the incoming one. The lower bound in the monochromatic limit is given by

$$\mathcal{T}=1-2\frac{\gamma_1}{\gamma}+\left(\frac{\gamma_1}{\gamma}\right)^2, \tag{3.12}$$

which is $4/9\approx 0.44$ in the example. There is an intermediate regime $\gamma_0<\Omega<10\gamma_0$ where the transmittance changes rapidly and it is noticeably smaller for a Fock-state pulse than for a coherent state. Finally, short light pulses, $\Omega\gg\gamma_0$, pass through the atom almost without being appreciably affected, realizing a sort of short-pulse filter. A simple explanation is that a large spectral part of a broadband pulse is far away from the atomic resonance, which reduces the effective coupling strength. Figure 1, therefore, suggests that in situations where temporal resolution is required, for example in a detection scheme, the best choice for the bandwidth is $\Omega\approx\gamma_0$ where relatively short light pulses still experience significant attenuation. Longer pulses provide less temporal resolution without much improvement of the signal, whereas shorter pulses experience a significantly smaller change.

Let us note briefly that the part of the impinging pulse that is not transmitted, is either reflected or, most probably, scattered in the transverse lossy modes. The reflectance has an upper bound, which is reached again in the monochromatic limit. It is $(\gamma_1/\gamma)^2=1/9\approx 0.11$ in the numerical example considered for Fig. 1, that is at least with probability 4/9 the photon is lost from the waveguide.

Due to saturation, there is a nonlinear effect in the transmittance. The more photons the light pulse carries, the more the atom gets excited. Population in the upper state of the atom reduces effectively the dipole strength, as follows from the term $\langle\sigma_z\rangle$ in the Eq. (3.4), which amounts, therefore, to a decrease in the amount of scattering. This effect is exhibited in Fig. 2 where the transmittance is plotted against the mean photon number N_a of the initial coherent-state pulse for various pulse bandwidths. Parameters are the same as in Fig. 1. The starting points of the curves at $N_a=1$ correspond to four different points on the curve of Fig. 1. For longer pulses, see the curve (i) or (ii) in the figure, the saturation effect is small. This is because the effective coupling strength $g_{\rm eff}$ decreases with the pulse length. Or, alternatively, one can view the same effect as a consequence of the photons arriving more distributed in time. For short pulses, on the other hand, the coupling constant becomes large enough to reach saturation even with weak incident light pulses. For example, curve (iii) corresponding to $\Omega=\gamma_0$ manifests a drastic nonlinear behavior even for photon numbers around 1.

Figure 3 shows transmitted and reflected photon numbers for $\Omega=\gamma_0/10$ [same as in curve (ii) of Fig. 2] depending on the mean photon number of the pulse. The square root of the mean photon number is shown with error bars, representing the inherent quantum noise associated with coherent states. In order to detect the single-atom scatterer with high probability, the change in the photon number (reflected or transmitted) must be larger than the noise. The figure reveals the minimum necessary photon number of the probe pulse to achieve the required operation regime. Photon numbers at about 20 in the probe pulse are sufficient to get a high quantum efficiency for the detector.

D. Phase shift and pulse deformation

When the carrier frequency is detuned from atomic resonance, the pulse can undergo a phase shift (dispersive scat-

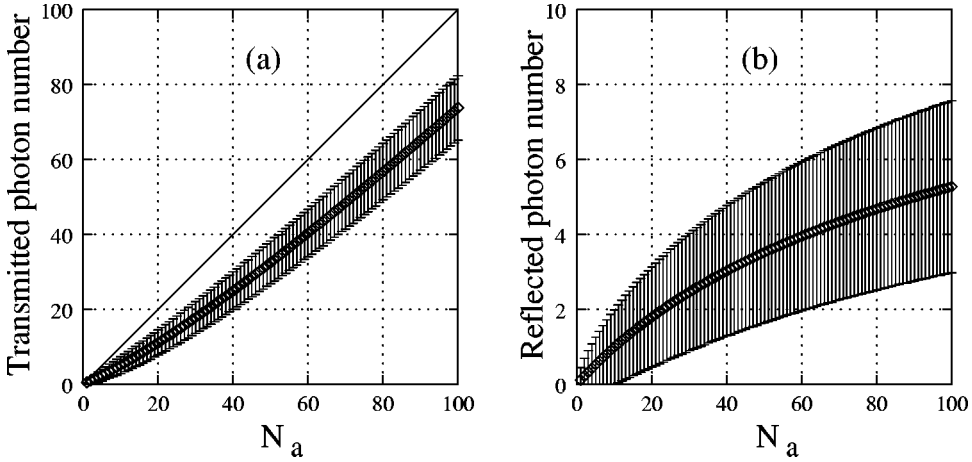

FIG. 3. Transmitted (a) and reflected (b) number of photons as a function of the initial mean photon number N_a. Error bars indicate the square root of the mean signal corresponding to the noise in a coherent state. The bandwidth is set $\Omega=0.1\gamma_0$.

tering). This phase shift can be the basis of a single-atom birefringence in waveguides. This happens if the atomic dipole is parallel to one of the polarization modes and orthogonal to the other one. Only the first polarization mode experiences a phase shift whose magnitude will be estimated, based on Eq. (2.15), in this section.

Strictly speaking the study of the phase properties necessitates the definition of a phase operator and the investigation of its time evolution. Here we will adopt a simplified treatment that allows perhaps a more instructive insight into the phase properties. Initially a coherent-state pulse, defined in Eq. (3.8), is taken with the phase 0, i.e., the amplitude of all the components is real. We assume that the state stays almost a coherent state all along the evolution. This is fulfilled when the pulse induces little atomic population excitation. Then, formally, the inversion operator σ_z can be replaced by $-1/2$ times the unity operator, and the state $|\Psi_0\rangle$ is indeed an eigenstate of the electric field operator, Eq. (2.15), at any time. The phase can be described by the argument of the corresponding complex eigenvalue, which we can write as

$$E^{(+)}(\tau)|\Psi_0\rangle = i\sqrt{\frac{\hbar\omega_0}{4\pi\epsilon c\mathcal{A}}}e^{-i\omega_0\tau}\alpha_0(\tau)(1+h(\tau))|\Psi_0\rangle, \tag{3.13}$$

where $\alpha_0(\tau)=\sqrt{N_a}(2\pi\Omega^2)^{1/4}\exp(-\Omega^2\tau^2/4)$ describes the initial Gaussian pulse shape. The radiated and the backscattered terms, the third and the fourth terms in Eq. (2.15), vanish because of the choice of the initial condition. The noise term is negligible as it is proportional to the atomic excitation, which is supposed to be small. Thus, the term $h(\tau)$ stems exclusively from forward scattering. It can be generated in a simple form by changing the integration variable in Eq. (2.15) as $t'\to\tau+z_A/c-t'$. One gets

$$h(\tau)=-\frac{1}{2}\frac{\sigma_A}{\mathcal{A}}\gamma_0\int_0^{\tau+z_A/c}dt'\exp[i(\omega_0-\omega_A)t'] \times\exp[-(\gamma-\Omega^2\tau/2)t']e^{-\Omega^2t'^2/4}. \tag{3.14}$$

On inspecting Eqs. (3.13) and (3.14), two effects of the forward scattering on the coherent-state amplitude can be noticed. First of all, the coherent-state amplitude is shifted with a relative amount of $h(\tau)$. Second, this shift depends on $\tau=t-z/c$, which yields a deformation with respect to the initial Gaussian pulse shape. The upper integration bound in Eq. (3.14) can be extended to infinity if the distance z_A between the initial pulse and the atom is very large compared to the pulse extension c/Ω. Hence, the only dependence on τ derives from the term $\gamma-\Omega^2\tau/2$ in the exponent. As τ varies within $\pm 1/\Omega$ in the pulse, the ratio of γ and Ω decides how much the pulse shape is distorted.

For very long pulses (quasimonochromatic excitation limit) the exponential decay with γ dominates the integrand. The other exponentials can be neglected and the integral renders the well-known Lorentzian form of the single-atom susceptibility $\chi=(\sigma_A/2\mathcal{A})/[(\omega_0-\omega_A)+i\gamma]$. Evidently, in this limit the result does not depend on τ. For general relation between Ω and γ, the integral has to be evaluated numerically. Let us first study the change of the coherent-state amplitude as a function of the detuning, and then its dependence on τ.

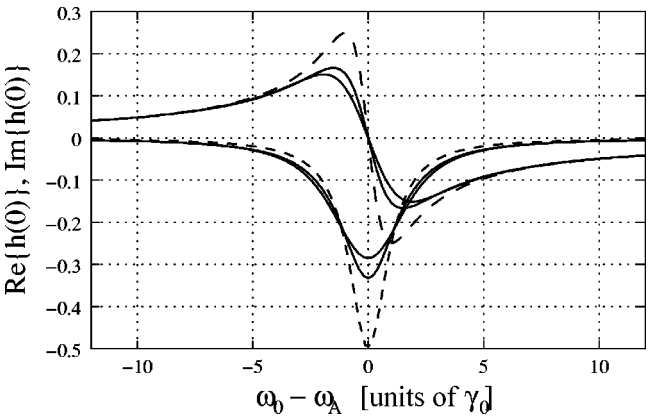

FIG. 4. Change of the coherent-state amplitude as a function of the pulse-carrier frequency detuning from the atomic resonance. Both the "absorption" Re$\{h(0)\}$ and the "dispersion" Im$\{h(0)\}$ curves are plotted with solid lines for $\Omega=\gamma_0$ and $\Omega=0.1\gamma_0$. This latter corresponds to the larger $h(0)$ values. Dashed curves show the Lorentzian shape for reference.

For the first case, we fix $\tau=0$ and plot the numerical solution of $h(\tau=0)$ in Fig. 4. We show the real and the imaginary parts of $h(0)$ as a function of the detuning $\omega_0-\omega_A$ for two bandwidth values, $\Omega=\gamma_0$ and $\Omega=0.1\gamma_0$. By analogy with the susceptibility, the real and imaginary parts can be regarded as an absorption and a dispersionlike curve, respectively. For reference, the Lorentzian function associated with the quasimonochromatic excitation limit (linewidth γ, oscillator strength $\sigma_A/2\mathcal{A}$) is also plotted with dashed lines. The three curves merge asymptotically for very large detunings. The reason is that the frequency components of the pulse are more or less uniformly detuned from the atomic frequency, much like in the monochromatic limit. Hence, the phase shift can be well approximated from the analytic Lorentzian solution. Otherwise, for moderate detunings, the bandwidth dependence of the change in the coherent-state amplitude is quite apparent in the figure. The narrower the

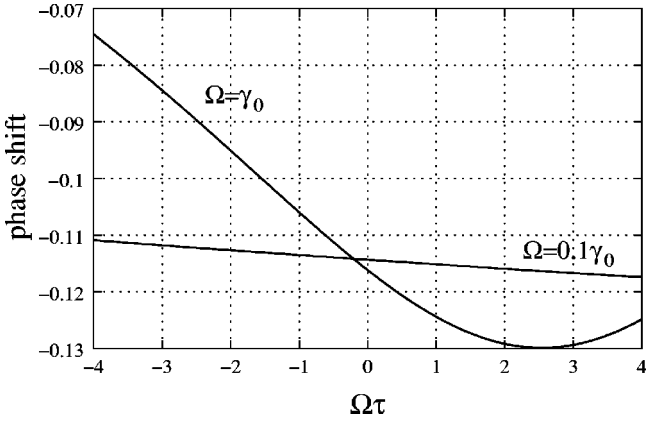

FIG. 5. Phase shift as a function of the pulse position $\Omega\tau$. For narrow enough bandwidth the phase shift gets independent of τ. Parameters are $\omega_0-\omega_A=4\gamma_0$, $\sigma_A/\mathcal{A}=1$.

bandwidth, the larger the phase shift obtained.

When the change in the coherent-state amplitude $h(\tau)$ is small with respect to 1 and approximately proportional to i, that is, for $\omega_0-\omega_A \gg \gamma_0$, it directly gives the rotation angle in phase space, i.e., the phase shift. The phase shift as a function of τ is presented in Fig. 5. The detuning is chosen $\omega_0-\omega_A=4\gamma_0$ where the absorption is well reduced and the pulse power is almost completely transmitted through the atom. One can see in the figure that rotation angles in the range of 0.11 rad$\approx 6°$ are induced by a single atom for $\sigma_A=\mathcal{A}$. Note that for $\Omega=0.1\gamma_0$ the phase shift is almost uniform, while it changes considerably for $\Omega=\gamma_0$. In both cases the deformation is asymmetric, showing that the front and the back of the pulse interact with an atom in a different state.

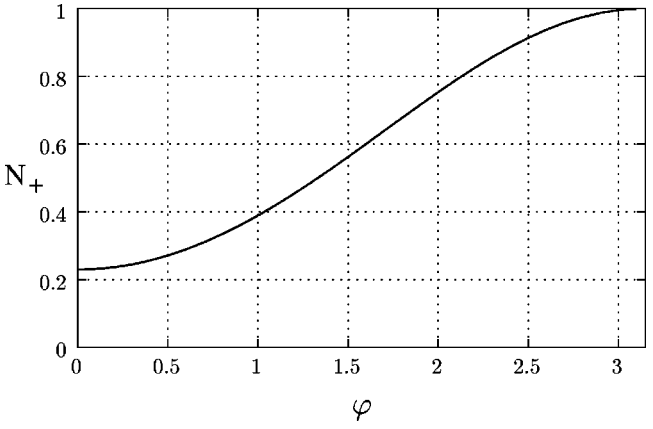

FIG. 6. Mean photon number N_+ outgoing in the $+z$ direction as a function of the relative phase φ of two identical counterpropagating coherent-state pulses. The mean photon numbers are $N_a=N_b=1$, the bandwidth is $\Omega=0.3\gamma_0$, and $\sigma_A/\mathcal{A}=1$.

IV. INTERFERENCE OF LIGHT PULSES

One possible application of such a setup is nonlinear photonics, i.e., doing optics with few photons beyond beam splitters and mirrors [19]. As a prototype of this dynamics, let us study now the ''collision'' of two pulses propagating in opposite directions. Instead of considering the modes $b_\omega(t_0)$ initially in vacuum state, we will properly define an initial state that describes a wave packet centered at $z=2z_A$. Then, this backward propagating wave packet and the forward propagating one encounter in the position of the atom at $z=z_A$, where the atomic dipole can mediate an interaction between them. The calculations are based on the general result presented in Eq. (2.15), which holds for any initial condition.

We calculate the Poynting vector in the range $z>z_A$ after the pulse collision. Here the field is composed of the initial pulse in the modes a_ω and its forward-scattered part, superimposed with the backscattered part of the pulse in the modes b_ω. One gets an expression quite similar to the result in Eq. (3.4)

$$S(\tau)=\frac{\Omega}{\sqrt{2\pi}}e^{-\Omega^2\tau^2/2}\Bigg[\langle u(\tau)|u(\tau)\rangle+\frac{\sigma_A}{2\mathcal{A}}\gamma_0\int_0^{\tau+z_A/c}dt'\,2\,\mathrm{Re}\{\mathcal{F}(\tau,t')\langle u(\tau)|2\sigma_z(t')|v(t'-z_A/c)\rangle\}$$
$$+\left(\frac{\sigma_A}{2\mathcal{A}}\gamma_0\right)^2\int_0^{\tau+z_A/c}dt'\,\mathcal{F}^*(\tau,t')\int_0^{\tau+z_A/c}dt''\mathcal{F}(\tau,t'')\langle v(t'-z_A/c)|4\sigma_z(t')\sigma_z(t'')|v(t''-z_A/c)\rangle\Bigg], \quad (4.1)$$

just we needed to introduce a second state $|v(t)\rangle$, which is defined by

$$|v(t)\rangle=(2\pi\Omega^2)^{-1/4}e^{\Omega^2t^2/4}[a_0(t)+e^{2i\omega_0z_A/c}\times b_0(t+2z_A/c)]|\Psi_0\rangle. \quad (4.2)$$

Let us consider first the case when the two counterpropagating pulses are in a coherent state. The initial state is composed of the state $|\psi_a\rangle$ as defined in Eq. (3.8), while the back-propagating modes are in the state $|\psi_b\rangle$ where

$$b_\omega(t_0)|\psi_b\rangle=\sqrt{N_b}e^{i\varphi}\left(\frac{2}{\pi\Omega^2}\right)^{1/4}\times\exp[-(\omega-\omega_0)^2/\Omega^2]e^{2i\omega z_A/c}|\psi_b\rangle. \quad (4.3)$$

The last exponential term ensures that the position of the pulse is $z=2z_A$ at $t=t_0$. The state $|v(t)\rangle$ is proportional again to the initial state

$$|v(t)\rangle=(\sqrt{N_a}+e^{i\varphi}\sqrt{N_b})|\Psi_0\rangle. \quad (4.4)$$

One can immediately recognize that the appearance of the state $|v(t)\rangle$ in the second and third terms of Eq. (4.1) gives rise to intriguing interferometric phenomena. Compared to the simple scattering scenario given by Eq. (3.4), the second term, which is responsible for the absorption, can be enhanced. To this end, the counterpropagating pulses must have the same phase, i.e., $\varphi=0$. Then the forward-scattered pulse and the backscattered pulse interfere constructively yielding a reduced transmitted signal. On the other hand, the two pulses can interfere destructively when they black out each other in the position of the scatterer, i.e., for $N_a=N_b$ and $\varphi=\pi$. The atom being in dark, this situation looks as if the

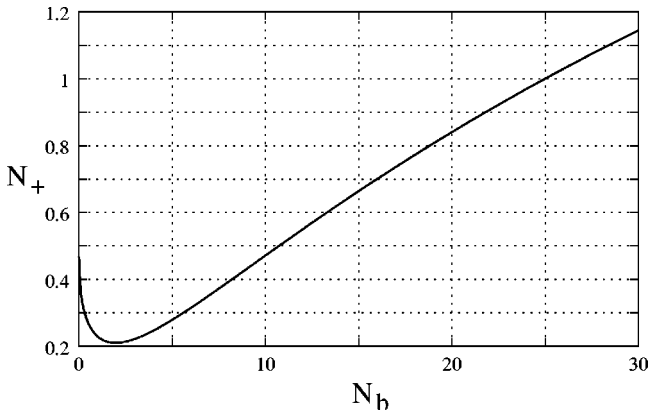

FIG. 7. Mean photon number N_+ outgoing in the $+z$ direction as a function of the mean photon number N_b of the pulse incoming from the backward $-z$ direction. Parameters are as in Fig. 6.

atom were absent and the pulses propagate freely. This simple example demonstrates that there is indeed a nontrivial interaction between the pulses mediated by a single atom. Since the transverse scattering is missing, the outcome is definitely different from the coherent sum of the outcomes obtained with two single pulses. In between the extreme cases the outgoing mean photon number in the $+z$ direction, denoted by N_+ varies as a function of the phase φ. This is shown in Fig. 6 where a difference of almost 80% is obtained for a bandwidth $\Omega=0.3\gamma_0$ and a beam cross section $\sigma_A/\mathcal{A}=1$.

Assume that we have a mean photon number N_a fixed, e.g., $N_a=1$. Then the photon number N_+ outgoing in the forward $+z$ direction can be tuned by varying the photon number N_b. This effect is represented in the Fig. 7. The well-pronounced minimum results from the concurrence of the second term of Eq. (4.1), which scales as $\sqrt{N_b}$ and reduces the outgoing photon number, and the third term, which is linear in N_b and increases the photon flux due to backscattered light. The manifest deviation from the linear behavior is due to atomic saturation.

Let us finally consider the collision of two Fock-state pulses on the atom. The initial state is $|\Psi_0\rangle=|1_a\rangle|1_b\rangle|g\rangle|0_e\rangle$, where $|1_b\rangle$ is defined by

$$|1_b\rangle=\int_0^\infty d\omega\left(\frac{2}{\pi\Omega^2}\right)^{1/4}\times\exp[-(\omega-\omega_0)^2/\Omega^2]e^{2i\omega z_A/c}b_\omega^\dagger(t_0)|0_b\rangle. \tag{4.5}$$

Initially there is no quantum correlation between the two Fock-state wave packets. As the phase in Fock states is completely undefined, one expects that the interference is missing in this case. This is true and can be formally traced back to the fact that for the auxiliary state of Eq. (4.1),

$$|v(t)\rangle=|0_a,1_b\rangle+|1_a,0_b\rangle, \tag{4.6}$$

the contribution of $a_0(t'-z_A/c)$ (''forward-scattered photon'') and the contribution of $b_0(t'+z_A/c)$ (''back-reflected photon'') do not add up algebraically. Note that for coherent-state pulses this was different, the second ''absorption'' term of Eq. (4.1) got a factor $\sqrt{N_a}+e^{i\varphi}\sqrt{N_b}$ and the Bloch equations had to be solved only for the mean of atomic operators. Here, for Fock states, one has to solve a specific realization of the generalized Bloch equations (see the Appendix). However, these equations are inhomogeneous and the solution is far from being the sum of two terms, one originating in $|0_a,1_b\rangle$ and the other in $|1_a,0_b\rangle$. The numerically obtained result for the mean photon number outgoing in the $+z$ direction is, however, very similar to the one obtained with one single impinging pulse. No interferometric enhancement or reduction of the outgoing photon number can be observed for pulses initially in Fock states.

V. CONCLUSION

For a field transversally confined in a tiny waveguide, a single atom is able to have a significant effect on a light wave packet traveling across the atom. As limiting cases of the time-dependent 1D scattering, one finds a transmittance reduction below 50%, strong nonlinearity in the transmittance even for very low energy pulses, and interferometric coupling of two wave packets with a visibility of up to 80%. All these effects clearly demonstrate that miniaturized waveguides or fibers coupled to an atomic dipole can be used as efficient single-atom detectors, or photon-photon couplers. As one might be able to control a single-atom state on the quantum level, this could pave the way to genuine quantum devices for optics, as, e.g., a quantum switch for light [20]. Similarly one could envisage to construct single-photon Bell state analyzers, as they would be needed for improved quantum cryptography or quantum teleportation setups.

In our model, we aimed at studying the fundamental nature of the interaction of a single atom with a waveguide field. A regime that can be referred to as ''strong-coupling regime'' occurs when the transverse extension of the waveguide modes is close to the single-atom radiative cross section. The coherent interaction between the field and the atom can dominate damping. In contrast to cavity QED, however, the waveguide-atom coupling yields a dissipationlike evolution of the atom since the waveguide modes form a broadband continuum, similar to the reservoir composed of the free-space radiation modes. On one hand, a single atom within the waveguide field becomes a significant scatterer, as featured by the effects presented in the paper. On the other hand, it is questionable if a weak quantum field can perform coherent population transfer in an atom. This is because a large effective single-atom Rabi frequency (g_{eff}) is accompanied by the presence of a large damping rate (γ_1) in the Bloch equations. In addition to this, the Rabi frequency depends on the interaction time defined by the pulse length. For example, for adiabatic passage techniques long interaction time is required, which inevitably leads to the reduction of the coupling constant. Our model equations provide a suitable ground to further study the dynamics of atoms coupled to one-dimensional continua of modes.

ACKNOWLEDGMENTS

We thank Jörg Schmiedmayer and Ron Folman for motivating this research by their interest in constructing single-atom detectors. We also thank Peter Zoller for stimulating discussions. This work was supported by the Austrian Science Foundation FWF (Project No. P13435). P.D. acknowledges the financial support by the National Scientific Fund of Hungary under Contract Nos. T034484 and F032341.

APPENDIX: DERIVATION OF VARIOUS MATRIX ELEMENTS OF THE ATOMIC OPERATORS

We prove in this appendix that the free-pulse operator $a_0(t-z_A/c)$ commutes with the population inversion operator $\sigma_z(t')$ for times $t>t'$. This lemma allows the derivation of a closed set of linear differential equations for the required matrix elements of the population inversion operator and for that of the two-time product $\sigma_z(t)\sigma_z(t')$. We briefly present these equations, which are formally very similar to the Bloch equations, and the ones obtained by the quantum regression theorem in the case of driving an atomic dipole transition with a classical field.

By definition

$$\begin{aligned} C &\equiv [a_0(t_1-z_A/c),\sigma_z(t_2)] \\ &= \int d\omega \exp[-i(\omega-\omega_0)(t_1-z_A/c)][\hat{a}_\omega(t_0),\sigma_z(t_2)] \\ &= \int d\omega \exp[-i(\omega-\omega_0)(t_1-z_A/c)]\Big\{[\hat{a}_\omega(t_2),\sigma_z(t_2)] \\ &\quad - g_\omega e^{-i\omega z_A/c}\int_0^{t_2} dt' e^{i(\omega-\omega_A)t'}[\sigma_-(t'),\sigma_z(t_2)]\Big\}, \end{aligned} \tag{A1}$$

where in the second step we used Eq. (2.8). Atomic and field operators, taken at the same time, commute, hence the first term vanishes. In the second term one can change the order of the integrals

$$\begin{aligned} C &= -e^{-i\omega_0 z_A/c}\int_0^{t_2} dt' \exp[i(\omega_0-\omega_A)t'] \\ &\quad \times[\sigma_-(t'),\sigma_z(t_2)]\int d\omega g_\omega \exp[-i(\omega-\omega_0)(t_1-t')]. \end{aligned} \tag{A2}$$

The coupling constant g_ω being a slowly varying function of ω around the given optical frequency ω_0 can be taken out of the integral. The remaining inner integral amounts to a Dirac-delta function and

$$\begin{aligned} C &= -e^{-i\omega_0 z_A/c}\int_0^{t_2} dt' \exp[i(\omega_0-\omega_A)t'] \\ &\quad \times[\sigma_-(t'),\sigma_z(t_2)]2\pi g_{\omega_0}\delta(t'-t_1) \\ &= -2\pi g_{\omega_0} e^{-i\omega_0 z_A/c}\exp[i(\omega_0-\omega_A)t_1] \\ &\quad \times[\sigma_-(t_1),\sigma_z(t_2)]\Theta(t_2-t_1), \end{aligned} \tag{A3}$$

where Θ is the Heaviside step function, which proves our conjecture.

The time-dependent effect of the light pulse on the atomic-dipole operators can be determined from the Eq. (2.12). Depending on the initial state of the pulses, various matrix elements have to be calculated and inserted in the expressions for the Poynting vector Eqs. (3.4), (3.7), and (4.1). In all the present cases, the required variables obey a set of linear differential equations that can be written in the form

$$\dot{\mathbf{s}} = \mathbf{B}\cdot\mathbf{s}+\mathbf{b}. \tag{A4}$$

When the initial pulses are in coherent states, the evolution of the quantum mean of the population inversion operator is needed. It can be obtained by integrating the above differential equation with

$$\mathbf{s} = \begin{pmatrix} \langle\hat{\sigma}_z\rangle \\ \mathrm{Re}\{\langle\hat{\sigma}'_+\rangle\} \\ \mathrm{Im}\{\langle\hat{\sigma}'_+\rangle\} \end{pmatrix}, \quad \mathbf{b} = \begin{pmatrix} -\gamma \\ 0 \\ 0 \end{pmatrix},$$

$$\mathbf{B} = \begin{pmatrix} -2\gamma & -2(\sqrt{N_a}+\sqrt{N_b}\cos\varphi)g(t) & 2\sqrt{N_b}\sin\varphi g(t) \\ 2(\sqrt{N_a}+\sqrt{N_b}\cos\varphi)g(t) & -\gamma & \omega_0-\omega_A \\ -2\sqrt{N_b}\sin\varphi g(t) & \omega_A-\omega_0 & -\gamma \end{pmatrix}, \tag{A5}$$

where

$$\hat{\sigma}'_+(t) = \hat{\sigma}_+(t)e^{i\omega_0 z_A/c}\exp[-i(\omega_0-\omega_A)t]. \tag{A6}$$

Formally, this equation is equivalent to the Bloch equations obtained for an atom driven by a classical time-dependent excitation. The corresponding single-photon Rabi frequency reads

$$g(t) = g_{\mathrm{eff}}\exp\left[-\frac{1}{4}\Omega^2(t-z_A/c)^2\right], \tag{A7}$$

with $g_{\mathrm{eff}}=g_{\omega_0}(2\pi\Omega^2)^{1/4}$.

The two-time averages in Eq. (3.4) can be obtained by using the quantum regression theorem. For a fixed time t' prior to time t, the variables

$$\mathbf{s}(t)=\begin{pmatrix}\langle\hat{\sigma}_z(t)\hat{\sigma}_z(t')\rangle\\ \langle\mathrm{Re}\{\hat{\sigma}'_+(t)\}\hat{\sigma}_z(t')\rangle\\ \langle\mathrm{Im}\{\hat{\sigma}'_+(t)\}\hat{\sigma}_z(t')\rangle\end{pmatrix} \tag{A8}$$

obey the linear differential equation given in the Eq. (A4) with $\mathbf{b}^T=(-\gamma\langle\sigma_z(t')\rangle,0,0)$.

When the counterpropagating pulses are initially in single-photon Fock-states, the matrix element $\langle 0_a,1_b|\sigma_z(t')|1\rangle$, where $|1\rangle=|0_a,1_b\rangle+|1_a,0_b\rangle$, is needed. For symmetry reasons, the required element is just the half of $\langle 1|\sigma_z(t')|1\rangle$, which can be obtained from the solution of Eq. (A4) with

$$\mathbf{s}(t)=\begin{pmatrix}\langle 1|\hat{\sigma}_z|1\rangle\\ \mathrm{Re}\{\langle 0|\hat{\sigma}'_-|1\rangle\}\\ \mathrm{Im}\{\langle 0|\hat{\sigma}'_-|1\rangle\}\end{pmatrix},\quad \mathbf{b}=\begin{pmatrix}-\gamma\\ 2g(t)\\ 0\end{pmatrix},$$

$$\mathbf{B}=\begin{pmatrix}-2\gamma & -4g(t) & 0\\ 0 & -\gamma & \omega_0-\omega_A\\ 0 & \omega_A-\omega_0 & -\gamma\end{pmatrix}. \tag{A9}$$

Note that nondiagonal matrix elements are involved in this set of equations. One can easily see that closed sets could be derived with increasing number of equations for higher photon number states, i.e., the presented approach is suitable to describe many other initial states as well. Finally, one gets for the necessary two-time average

$$\mathbf{s}(t)=\begin{pmatrix}\langle 1|\hat{\sigma}_z(t)\hat{\sigma}_z(t')|1\rangle\\ \langle 0|\hat{\sigma}'_-(t)\hat{\sigma}_z(t')|1\rangle\\ \langle 1|\hat{\sigma}'_+(t)\hat{\sigma}_z(t')|0\rangle\end{pmatrix},\quad \mathbf{b}=\begin{pmatrix}-\gamma\langle 1|\sigma_z(t')|1\rangle\\ g(t)\\ g(t)\end{pmatrix},$$

$$\mathbf{B}=\begin{pmatrix}-2\gamma & -2g(t) & -2g(t)\\ 0 & i(\omega_0-\omega_A)-\gamma & 0\\ 0 & 0 & i(\omega_A-\omega_0)-\gamma\end{pmatrix}. \tag{A10}$$

[1] S. Stenholm, Opt. Commun. **123**, 287 (1996); P. Törmä and S. Stenholm, Phys. Rev. A **54**, 4701 (1996).

[2] P. G. Kwiat and H. Weinfurter, Phys. Rev. A **58**, R2623 (1998).

[3] P. W. H. Pinkse, T. Fischer, P. Maunz, and G. Rempe, Nature (London) **404**, 365 (2000).

[4] C. J. Hood, T. W. Lynn, A. C. Doherty, A. S. Parkins, and H. J. Kimble, Science **287**, 1447 (2000).

[5] A. Rauschenbeutel, G. Nogues, S. Osnaghi, P. Bertet, M. Brune, J. M. Raimond, and S. Haroche, Science **288**, 2024 (2000).

[6] M. Weidinger, B. T. H. Varcoe, R. Heerlein, and H. Walther, Phys. Rev. Lett. **82**, 3795 (1999).

[7] S. J. van Enk and H. J. Kimble, Phys. Rev. A **61**, 051802(R) (2000); **63**, 023809 (2001).

[8] M. D. Lukin and A. Imamoglŭ, Phys. Rev. Lett. **84**, 1419 (2000).

[9] P. Kochan and H. J. Carmichael, Phys. Rev. A **50**, 1700 (1994).

[10] C. W. Gardiner, Phys. Rev. Lett. **70**, 2269 (1993).

[11] H. J. Carmichael, Phys. Rev. Lett. **70**, 2273 (1993).

[12] G. Drobný, M. Havukainen, and V. Bužek, J. Mod. Opt. **47**, 851 (2000).

[13] M. Havukainen, G. Drobný, S. Stenholm, and V. Bužek, J. Mod. Opt. **46**, 1343 (1999).

[14] Q. A. Turchette, C. J. Hood, W. Lange, H. Mabuchi, and H. J. Kimble, Phys. Rev. Lett. **75**, 4710 (1995).

[15] M. W. Mitchell, C. I. Hancox, and R. Y. Chiao, Phys. Rev. A **62**, 043819 (2000).

[16] A. W. Snyder and J. D. Love, *Optical Waveguide Theory* (Chapman & Hall, London, 1991).

[17] K. J. Blow, R. Loudon, S. D. Phoenix, and T. J. Shepherd, Phys. Rev. A **42**, 4102 (1990).

[18] C. Cohen-Tannoudji, J. Dupont-Roc, and G. Grynberg, *Atom-Photon Interactions* (Wiley, New York, 1998).

[19] K. J. Resch, J. S. Lundeen, and A. M. Steinberg, Phys. Rev. Lett. **87**, 123603 (2001).

[20] K. M. Gheri and H. Ritsch, Phys. Rev. A **56**, 3187 (1997).

[21] For an atom within the waveguide, the lossy modes, not guided by the structure, compose the environment. These modes are continued into the free space radiation modes outside the material. For small numerical aperture the mode density of the lossy modes is close to the one in free space.